Published in final edited form as:
Anal Chem. 2011 March 15; 83(6): 2162–2171. doi:10.1021/ac103006b.

Pulsed Multiple Reaction Monitoring Approach to Enhancing Sensitivity of a Tandem Quadrupole Mass Spectrometer

Mikhail E. Belov*, **Satendra Prasad**, **David C. Prior**, **William F. Danielson III**, **Karl Weitz**, **Yehia M. Ibrahim**, and **Richard D. Smith**
Biological Sciences Division, Pacific Northwest National Laboratory, P.O. Box 999, Richland, Washington 99352, United States

Abstract

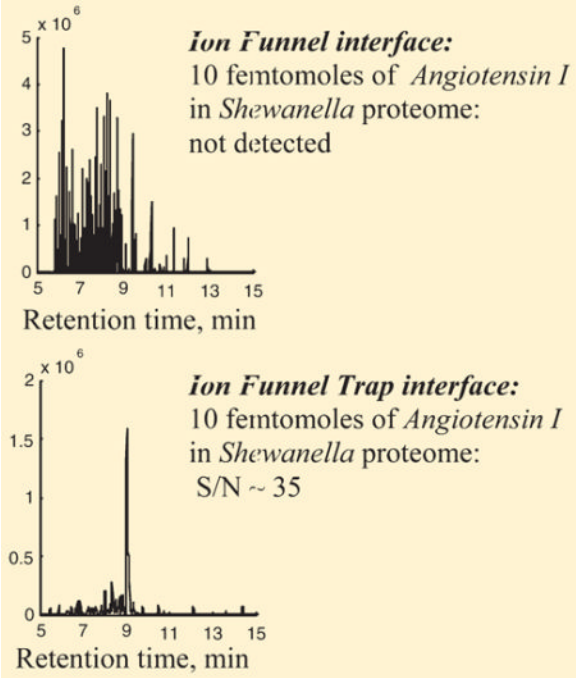

Liquid chromatography (LC)–triple quadrupole mass spectrometers operating in a multiple reaction monitoring (MRM) mode are increasingly used for quantitative analysis of low-abundance analytes in highly complex biochemical matrixes. After development and selection of optimum MRM transitions, sensitivity and data quality limitations are largely related to mass spectral peak interferences from sample or matrix constituents and statistical limitations at low number of ions reaching the detector. Herein, we report on a new approach to enhancing MRM sensitivity by converting the continuous stream of ions from the ion source into a pulsed ion beam through the use of an ion funnel trap (IFT). Evaluation of the pulsed MRM approach was performed with a tryptic digest of *Shewanella oneidensis* strain MR-1 spiked with several model peptides. The sensitivity improvement observed with the IFT coupled in to the triple quadrupole instrument is based on several unique features. First, ion accumulation radio frequency (rf) ion trap facilitates improved droplet desolvation, which is manifested in the reduced background ion

Corresponding Author: mikhail.belov@pnl.gov.

Supporting Information. Additional information as noted in text. This material is available free of charge via the Internet at http://pubs.acs.org.

noise at the detector. Second, signal amplitude for a given transition is enhanced because of an order-of-magnitude increase in the ion charge density compared to a continuous mode of operation. Third, signal detection at the full duty cycle is obtained, as the trap use eliminates dead times between transitions, which are inevitable with continuous ion streams. In comparison with the conventional approach, the pulsed MRM signals showed 5-fold enhanced peak amplitude and 2–3-fold reduced chemical background, resulting in an improvement in the limit of detection (LOD) by a factor of ~4–8.

There is an increasing emphasis in the ultrasensitive detection of multiple biomarkers, which maybe specific and diagnostic for a given clinical condition.[1,2] Though clinical application of a biomarker typically employs an antibody-based analytical approach, such as enzyme-linked immunosorbent assay (ELISA),[3] the multiple biomarker screening would incur nonspecific antibody–antigen binding and the associated cost of antibody production as more than one monoclonal antibody is needed per protein, each being required to recognize a separate epitope. The capability of tandem quadrupole mass spectrometry (MS/MS) to concurrently and with high specificity perform highly sensitive quantitative analysis of many trace constituents in highly complex matrixes has been well-recognized and increasingly employed in proteomics research.[4–7]

The essential requirement for triple quadrupole (QqQ) multiple reaction monitoring (MRM)[8,9] analysis is the ability to select specific *m/z* precursor ions (Q1), fragment these ions in a collision-induced dissociation experiment (q2), and then sequentially select and detect multiple specific *m/z* fragment ions (Q3), i.e., specific “transitions”. MRM analyses are limited by either sensitivity (i.e., signal intensity) or measurement selectivity (e.g., peak interferences due to the presence of other detected species of measurement background). Sensitivity of a QqQ instrument is highest when both Q1 and Q3 operate at fixed precursor and fragment ion *m/z* values. This regime, however, results in inability to detect the full mass spectrum and places part of the burden for confident identification on the separation stage preceding the MS, e.g., reversed-phase capillary liquid chromatography (RPLC).[10,11] A hybrid triple quadrupole–linear ion trap (Q-TRAP) has been shown to yield additional confidence in precursor ion identifications by rapidly switching from quadrupole MRM measurements to full MS/MS acquisitions with a linear ion trap.[12] Several modifications of the advanced MRM approaches have been reported,[13] including techniques when specific MRM transitions trigger either a full product scan with a Q-TRAP[14] or initiate detection of additional transitions with a QqQ instrument.[15] Another quantification approach employs the use of stable isotope labeling such as differentially labeled samples by amino acids [16] or internal labeled standards.[17] In a label-free MRM quantitative analysis, high RPLC peak capacity, reproducible retention times, and the presence of retention time markers are critically important for confident precursor ion identifications. A key benefit of RPLC is separation of analyte molecules from sample/matrix components of the same *m/z*, which would otherwise coelute and potentially cause ionization suppression in the electrospray ionization (ESI) source or lead to peak interferences at the detector. Efforts aimed at increasing sample throughput imply the use of shorter LC gradients, resulting in potential coelution of the targeted analytes with other components of the same *m/z*. If both the precursor and fragment ions of the analyte and other matrix ions overlap in the *m/z* domain, these components would cause peak interferences and contribute to increased chemical background, raising the limit of detection (LOD) due to this “chemical noise”. Removal of these interferences could be facilitated by an additional separation stage, such field asymmetric ion mobility spectrometry (FAIMS),[18,19] though compromised by the reduced sensitivity. In other cases characterized by the absence of peak interferences and the lack of statistically significant ion counts at the detector, increased signal peak amplitude would be beneficial for reliable quantitative analysis.

The implementation of higher pressure ion transmission devices such as the electrodynamic ion funnel (IF),[20,21] the related S-lens,[22] or an rf-only quadrupole ion guide,[23] have improved ion sampling and ion transport from an ESI ion source to an MS detector. An IF constitutes a stacked ring assembly of electrodes with progressively reduced diameters of the center apertures to interface to a multipole ion guide operating at lower pressure. In the IF, ions experience a direct current (dc) field superimposed on 180° phase-shifted rf waveforms applied to adjacent lenses. The rf electric field causes radial confinement of the ions, which would otherwise be lost radially due to space charge repulsion and diffusion. This device has been shown to efficiently confine and transport ions at pressures up to ~30 Torr.[24] In experiments with highly complex biochemical samples, not only the useful analyte ions but also partially desolvated charged molecules are efficiently transmitted by the IF, leading to proportionally higher levels of, e.g., chemical background.

We have shown that chemical background suppression is concurrently achieved with an increase in the analyte signal through the use of an ion funnel trap (IFT).[25,26] As compared to the more conventional quadrupolar 3D and linear 2D ion traps operating at pressures of 10^{-3} to 10^{-4} Torr, the IFT has been shown to provide efficient ion confinement, accumulation, and pulsed ejection at pressures of 1–5 Torr.[25–28] Importantly, this trap has been used only for ion accumulation, while detection was accomplished either with a time-of-flight mass spectrometer (TOFMS)[25,26] or an ion mobility (IM)-TOFMS.[27,28] This arrangement enables ion trap operation at elevated pressures. Since trapping efficiency is proportional to the number density of gas molecules,[29] accumulation of ions at elevated pressures (~1 Torr) in the IFT is more efficient than that in the conventional 3D quadrupolar ion trap under typical operating conditions (~10^{-4} to 10^{-5} Torr). Following accumulation, ions are ejected from the IFT as high-density donut-shaped packets and then confined to a smaller radius by the converging section of the IFT. This confinement occurs without ion losses, as immediately following the trap region ions begin to separate according to their mobilities, resulting in reduced Coulombic repulsion at any plane perpendicular to the trap axis. Three attractive characteristics of the IFT reported are the high trapping efficiency (~50%), high charge capacity (~3 X 10^7 elementary charges), and high duty cycle (~95%). The coupling of an IFT to a TOFMS yielded a 10–30-fold gain in signal to noise (S/N) when compared to the continuous mode of operation.[25,26] This improvement was, in part, attributed to a decrease in the chemical background levels facilitated by desolvation of ion clusters in the rf heating environment.

To further increase sensitivity of a QqQ instrument operating in the MRM mode, we have introduced an IFT prior to the MS stage. This transforms the conventional continuous mode of operation to a pulsed mode and requires somewhat different approaches to understanding ion selection and detection. Our initial evaluation with a complex bacterial proteome revealed that the capillary LC–pulsed MRM approach yields significantly reduced chemical background, increased MS signal amplitude, and full ion utilization duty cycle. The latter is important for short MRM dwell times, such that acquisition periods are comparable or shorter than the switching time (or “dead time”) between transitions. In all, the IFT combination with QqQ MRM measurements provides significant gains in achievable LOD due to improved measurement sensitivity and higher S/N.

EXPERIMENTAL SECTION

Chemicals and Materials

Lyophilized kemptide, angiotensin I, syntide 2, bradykinin, leucine enkephalin, dynorphin A porcine 1–13, neurotensin, and fibrinopeptide A were purchased from Sigma-Aldrich (St. Louis, MO). These were serially diluted to prepare concentrations ranging from 0.25 to 500

nM peptides in 0.25 mg/mL tryptic digest of *Shewanella oneidensis* strain MR-1 proteins and 0.01 mg/mL tryptic digest of bovine serum albumin.

Ion Funnel Trap

Design of both the IF and IFT has been described elsewhere,[21,25,27] and only a brief outline is reported here. A two-dimensional cross section of an assembled IFT is shown in Figure 1A. Each electrode in the IFT was energized with an rf waveform using a custom-built rf generator. The waveform on the adjacent plates was 180 phase-shifted, 60–70 V peak to peak in amplitude, and at a frequency of ~0.6 MHz. The dc gradient in the nontrapping sections of the IFT was maintained at 27 V/cm, whereas the dc gradient in the trap section was kept at 4 V/cm to maximize the trapping efficiency. Pulsed potentials were applied to entrance and exit grids (95% transmission) to accumulate ions for a predetermined time. Ions were released from the trap in 500 μs pulses that was synchronized with the second resolving quadrupole (Q3) scan.

Synchronizing the Ion Funnel Trap with Q3

Figure 1, parts A and B, shows a schematic of the instrument used in this study. All experiments were performed with a triple-stage quadrupole analyzer TSQ Quantum Ultra (Thermo Fisher Scientific, San Jose, CA). Operation of the IFT in the MRM analysis required synchronization between an ion release and Q3 scan events which is summarized in Figure 1B. During an MRM analysis, the Q3 exhibits a cyclic process of transmitting specific fragment ions (or transitions) for short periods or dwell time over a narrow *m/z* window. When using the IFT, an ion release event was delayed with respect to the start of a Q3 scan. This delay accounts for an ion packet transit time from the IFT exit grid to the Q3 entrance and ensures the arrival time of the ion packet to be in the middle of the Q3 scan. Importantly, since the ion packet temporal profile (<5 ms) is shorter than the Q3 scan duration (<10 ms), all the transmitted ions would represent a narrow peak in the middle of the Q3 scan, despite the *m/z* width of the Q3 scan. Given scan duration of ~10 ms and an *m/z* range of ~0.002 Da, i.e., under typical MRM conditions, the pulsed mode of operation would still yield a narrow peak in the middle of the *m/z* range. Though Q3 transmits only a narrow *m/z* range, an ion packet traverse time across the Q3 is shorter than the scan time (or averaging time), being reflected in the peak line shape at the detector. Another important feature of the pulsed MRM approach is independence of the delay time on *m/z* of a specific transition. Since ion packet transit times from the IFT exit gate to the Q3 entrance were similar for different precursor ions used in the experiments, only one delay time for a given accumulation time was used throughout LC–MRM study for all the transitions. This feature drastically simplifies experimental setup and makes the approach amenable to analysis of an arbitrary number of transitions.

The synchronization pulse was fed from the TSQ instrument and routed into a digital input/output NI USB-6221 card (National Instruments, Austin, TX) for triggering a digital waveform, which, in turn, was supplied to the input of a custom-built voltage amplifier. Two independent channels of the voltage amplifier were used to control both the IFT entrance and exit gates.

The use of an IFT also allows seamless switching to the continuous mode of operation that is equivalent to operation of an IF. This capability was enabled by maintaining potential levels at both entrance and exit grid at constant values corresponding to the optima for ion transmission through the trap region.

A number of experimental parameters were examined in the experiments with the IFT. These include pulsed voltage amplitudes, which were applied to the entrance and exit grids,

varying *m/z* transmission window from 2 mDa to 2 Da, the dwell time from 2 to 40 ms, and delays between the ion release event and Q3 scan. Since ions were accumulated in the trap during an MRM (and MS/MS) analysis, the dwell time was equivalent to accumulation time in the trap plus the switching time between transitions (or the dead time) measured to be equal to 4 ms for the TSQ instrument.

LC–MRM

The tryptic digest of *S. oneidensis* strain MR-1 proteins containing spiked peptides was analyzed with a custom-built high-performance liquid chromatograph (HPLC) equipped with two columns and an autosampler (CTC Analytic, Switzerland). The components of the HPLC system used here are identical to that described in an earlier publication.[30] Aliquots (5 μL) of the samples were loaded onto an LC column that was 15 cm × 75 μm i.d. fused-silica capillary (365 μm o.d., Polymicro Technologies, Phoenix, AZ), packed with 3 μm C18 packing material (300 Å pore size, Phenomenex, Torrance, CA). A constant pressure of 5000 psi was maintained during the 30 min gradient where mobile phase composition was varied exponentially from 99% of 0.1% formic acid in nanopure water (mobile phase A) to 70% of 0.1% formic acid in acetonitrile (ACN) (mobile phase B). Electrospray-generated ions were sampled into the heated capillary–IFT interface and then introduced into the TSQ mass spectrometer as shown in Figure 1. The ion source conditions and the MS parameters were defined using Xcalibur 2.0.7 (Thermo Scientific, San Jose, CA). The three most intense fragments for every precursor ion were monitored where the fragmentation conditions (collision energy and collision cell pressure) were optimized in a separate direct infusion experiment. Transitions observed during direct infusion were verified using an in-house peptide fragmentation prediction algorithm. Parent ions and their corresponding fragments with optimum collision energies are listed in Supporting Information Table S1. Also included in the list were two peptides (m/z 703.98, *m/z* 1154.63) originating from tryptic digest of *S. oneidensis* strain MR-1 proteins. Signals arising from these endogenous peptides were used as retention time markers to align LC chromatograms and normalize LC retention times.

Sample Analysis and Data Processing

Analyses of samples included injections in the following order: mobile phase A (purge LC column), control sample (tryptic digest of *S. oneidensis* MR-1 proteins), and analytical sample (tryptic digest of *S. oneidensis* strain MR-1 proteins spiked with peptides). Each of the control and the analytical samples was analyzed in triplicate. Xcalibur 2.0.7 was used to visualize chromatograms from LC–MRM data sets. Selected ion chromatograms (SIC) of the endogenous peptides were used to normalize elution times peptides. The NET (±0.05 min) was used to assign identities to target peptides at LOD levels. Peaks were integrated using Xcalibur 2.0.7 by extracting SIC and manually defining retention times, peak widths (~8 s), and noise. Selected traces were exported into Matlab 2008a and aligned to a reference chromatogram using a correlation-optimized warping (COW) algorithm.[31]

RESULTS AND DISCUSSION

Chemical Noise Limited Cases with Skimmer and Electrodynamic Ion Funnel Interfaces

Prior to conducting LC–pulsed MRM experiments, we established baselines using both the commercial platform's capillary–skimmer and more advanced capillary–IF interfaces. Figure 2A shows an LC–MRM chromatogram acquired using the ion source equipped with the capillary–skimmer interface. Peaks in the chromatogram represent eight target peptides spiked into a tryptic digest of *S. oneidensis* strain MR-1 at equimolar concentrations of 100 nM. The trace shown in Figure 2A was used to determine elution times of the peptides over the 30 min chromatographic separation. The order of elution and characteristic retention

times are kemptide (1, 5.43 min), dynorphin A porcine 1–13 (2, 7.19 min), fibrinopeptide A (5, 8.01 min), neurotensin (6, 8.61 min), leucine enkephalin (7, 8.85 min), angiotensin I (8, 9.01 min), syntide 2 (3, 7.47 min), and bradykinin (4, 7.49 min). The latter two peptides coeluted as shown in the inset of Figure 2A. In the conventional capillary–skimmer arrangement, detection of ~50 fmol of target peptides loaded on the LC column was unreliable due to low analyte signal and interferences with high-abundance peaks from matrix constituents (Figure 2B, red trace). Replacement of the skimmer interface with an IF resulted in improved ion transport from the ion source to quadrupole analyzers. Signal enhancement of up to 6-fold was observed across total ion current chromatogram, TICs (Figure 2B, blue trace), which translated to ~7-fold improvement in S/N of the kemptide peak (Figure 2C, blue trace) when compared to that of the skimmer interface (Figure 2C, red trace). However, insignificant change in S/N was observed for target peptides which eluted in the regions of the LC gradient corresponding to the abundant matrix constituents (~6–9 min), as shown in Figure 2D. As an example, Figure 2E demonstrates the case with syntide 2 where a similar S/N value was observed with both skimmer and IF interfaces. This discrepancy could be explained by a proportional increase in both the analyte signal and chemical background level. The observed S/N improvement for the kemptide ions is consistent with this since it elutes from the chromatographic column before the high-abundance matrix components (Figure 2D). Improvements in S/N of dynorphin A porcine 1–13, fibrinopeptide A, leucine enkephalin, neurotensin, angiotensin I, and bradykinin peaks were found to be limited by the chemical background level when using the electrodynamic IF interface.

Inclusion of the IFT in LC–MS/MS Analyses

Initial experiments with the IFT were conducted in the MS/MS mode (2 *m/z* scan unit range for fragment ions), and efforts were focused on characterizing the gains in analyte signals due to ion accumulation during switching time for transitions (or “dead times”). Consequently, analyses were performed at sample concentrations that provided abundant analyte signals (~500 fmol). Figure 3 shows a comparison of LC–IF-MS/MS (Figure 3A) and LC–IFT-MS/MS (Figure 3B) results where the trap accumulation time was 14 ms. LC experiments were performed with 0.05% trifluoroacetic acid (TFA) added to both mobile phase A and B as an ion pairing agent. TICs were derived by integrating analyte signals from 24 transitions. Each LC peak was between 6 and 10 s wide (half-height), which resulted in an average of ~24 data points across each peak. When using the IFT, each data point along the LC chromatogram represents a single ion release for each transition monitored. Comparison of the traces shows an increase in the analyte signals across six of the peptides (excluding kemptide and dynorphin A porcine 1–13) with the use of the IFT as compared to the IF. An increase in the total ion signal with the IFT is correlated with an increase in the MS peak amplitude, which is shown for the three transitions of triply charged angiotensin I in Figure 3C: IFT (green trace) and IF (blue trace). It is important to note that in the IFT analyses, the variations in the mass spectral signals do not correspond to resolved peaks but actually are observed as narrower peaks in the middle of the *m/z* range for which they would normally be observed. This is due to the fact that the resident time of an ion packet in Q3 is shorter than the Q3 scan duration (10 ms). Direct measurements revealed that the temporal profiles of ion packets entering Q3 were typically shorter than 3 ms. Therefore, the mass spectral peaks obtained with IFT are convoluted with the temporal profiles for their respective ion packets traversing the Q3 quadrupole. The accumulation of ions and rapid ion ejection from the IFT produces spatially compressed ion packets of higher charge density, as reflected in the fragment peak amplitudes (Figure 3C). The areas under the MS peaks, which represent the total number of ions of a given type, are effectively conserved for both the IFT and IF measurements. Deviations from the exact match in the total number of ions in the two experiments in Figure 3 can be attributed to variations in ion

accumulation efficiencies in the IFT (~20–50%)[25,27] and by the "dead" time between transitions for the IF analyses (~40%). For instance, we observed that the peak integrals can be greater with IFT analyses compared to IF, particularly, for ions with higher trapping efficiencies such as fibrinopeptide A, bradykinin, neurotensin, and angiotensin I. Peptides (e.g., kemptide) which eluted off a chromatographic column prior to elution of the most abundant endogenous species were found to exhibit similar peak integrals in IF and IFT analyses.

To evaluate accumulation efficiencies of target analytes in the presence of a complex matrix we have run direct infusion experiments with a tryptic digest of bovine serum albumin (BSA) spiked with the reference peptides. The latter were added to a 160 nM BSA digest to produce two aliquots having 100 and 10 nM peptide concentrations. The complex mass spectrum in Supporting Information Figure S1A depicts a Q1 full scan obtained with the BSA tryptic digest spiked with 100 nM reference peptides. The mass spectrum is dominated by constituents from the BSA digestion. Following Q1 full scan experiments, MS/MS analyses of the reference peptides were performed. During these analyses, the IFT was filled with charged particles without any upstream ion filtering/selection. A total of 24 transitions were monitored in the continuous mode of operation (the IF regime) and in the trapping mode at accumulation times of 6, 8, 14, 24, 34, and 44 ms. In Supporting Information Figure S1B, results are summarized as a plot of intensity (MS peak amplitude) versus the trap accumulation time for a single fragment ofkemptide ions (m/z 567.33, b_5-NH3). An ~2.5-fold increase in peak amplitude was observed at an optimum accumulation time of 8 ± 1 ms (100 nM) and 14 ± 1 ms (10 nM) when compared to an MS spectrum where ions were not accumulated (IF). The gain is also reflected in the mass spectrum of *m/z* 567.33 (b_5-NH3) acquired with and without the trap function (Supporting Information Figure S1C) and is consistent with results observed for analysis of samples containing high concentrations of targeted peptides.

Two important points can be drawn from the data illustrated in Supporting Information Figure S1. First, reaching the maximum signal amplitude followed by a modest decrease in the amplitude of the reference peptides indicates that the IFT becomes filled to its capacity before the longer accumulation times. Therefore, the optimum ion accumulation time for the sample under investigation is approximately 8–15 ms. Second, similar dependences of the signal intensities on the accumulation time for the reference peptide at different concentrations (10 and 100 nM) strongly suggest that the observed amplitude decrease at longer accumulation times is caused by the general ion population rather than the reference peptides and also suggests that the IFT-QqQ instrument maintains signal response linearity in regard to the spiked peptide concentrations even at accumulation times longer than the optimum trapping time. The latter point was further investigated in the following LC–IFT-MRM experiments.

Enhanced S/N and LOD through Reduced Chemical Background

Figure 4 demonstrates direct comparison of the reference peptide analyses using LC–IF-MRM and LC–IFT-MRM approaches. As described in the Experimental Section, peptides were added to a 0.25 mg/mL tryptic digest of *S. oneidensis* proteome at concentrations ranging from 0.2 to 500 nM. MRM analyses were conducted with a total of24 transitions, using three most abundant transitions per precursor ion species. Each transition was monitored by scanning Q3 over a very limited *m/z* range (2 mDa) with the average dwell time varying from 2 to 40 ms. SICs of angiotensin I, syntide 2, bradykinin, and neurotensin were acquired in the continuous mode (IF) and trapping mode using 6 and 44 ms accumulation times in the IFT. When analyzed using the IF interface, angiotensin (10 fmol) and syntide 2 (40 fmol) were not detectable, whereas bradykinin and neurotensin peaks appeared at low S/N, mostly limited by the pronounced signals from matrix constituents. Ion

accumulation for 6 ms using the IFT interface led to angiotensin I and syntide 2 being detected at S/N of up to 12 (not detectable with the IF), whereas insignificant changes were observed for bradykinin and neurotensin peaks. Increasing ion accumulation time to 44 ms resulted in up to 10-fold signal loss across the SICs accompanied by pronounced reductions in the background levels. Overall, accumulation of ions at longer times in the IFT provided 6–30-fold enhancement of S/N across all the studied analyte peaks when compared to those obtained with the IF interface. A similar increase in the S/N was partially attributed to the reduced background levels, and was earlier observed in the experiments with IFT coupled to a TOFMS.[25,26] One plausible explanation for the observed improvement in the S/N ratios is a more efficient desolvation process in the IFT due to the extended residence time in conjunction with the additional rf heating at higher pressure, which contributes to chemical background reduction by, e.g., solvent cluster breakup and desolvation. Importantly, such reductions in background levels presumably occur at a much higher rates that the loss of analyte due to the overfilling of the trap. Therefore, despite the loss of analyte at longer accumulation times, the S/N ratios of the monitored peptides were found to further increase. This implies that the LOD in LC–IFT-MRM analyses can be improved over that obtained in the continuous mode ofoperation for the cases when quantitation is limited by the chemical background.

Crucially important for the LC–MRM analysis is the linearity of analyte signal response to the change in analyte concentration. In the course of LC–IF-MRM experiments, we have rigorously examined the analyte signal response as a function of the analyte concentration using reference peptides spiked into a tryptic digest of *S. oneidensis* MR-1 proteins. Signal abundances of all the reference peptides were derived using a total of 24 transitions at different accumulation times, and a short excerpt from this study is shown in Figures 5 and 6. Figure 5 illustrates the peak area and S/N for syntide 2 as a function of the peptide amount loaded onto the LC column in both LC–IF-MRM and LC–IFT-MRM studies. The latter was conducted at an ion accumulation time of 44 ms in the IFT. Each data point in Figure 4 represents the integrated signal for the three syntide 2 transitions recorded in separate LC experiments. Both the LC–IF-MRM and LC–IFT-MRM experiments revealed excellent linearity between the peak areas and moles of syntide 2 over the wide range of peptide concentrations. A surprising observation was that though the IF results displayed a steeper slope of the concentration curve, implying higher signal intensities and, presumably, sensitivity, the IFT experiments yielded an improved lower limit of quantitation (LOQ) and LOD. Figure 5B shows the S/N ratio for the data in Figure 5A as a function of the peptide amount loaded onto the LC column. The trends from Figure 5A are reversed in favor of the IFT results. Improvements in S/N for the IFT data strongly indicate that drastically reduced chemical background levels contribute to the overall sensitivity increase with the pulsed MRM approach. Such an increase in the LOQ/LOD is not limited to a single peptide but was, rather, observed for all the analytes of interest. To further illustrate this point, in Figure 6 we report both the signal intensities and MS transition signals at the LOD levels for the other peptide (angiotensin I) monitored in LC–IF-MRM and LC–IFT-MRM experiments. The inset in Figure 5A shows that the correlation between the peptide signal and loaded amount is not linear at less than 40 fmol for the IF study, which implies the integrated response at these levels of the spiked peptide was arising from matrix constituents and not from angiotensin I. This is supported in the SIC plot in Figure 6B at 20 fmol of angiotensin I, which shows the trace dominated by background signals. When analysis was repeated with the IFT interface (Figure 6D-F) the linearity was excellent down to 2.5 fmol (r^2 = 0.9957), as evident from the inset. In addition, the SIC (Figure 6E) showed reduced chemical background with an intense angiotensin I response (~9 min) and an improvement in the LOD by a factor of 8. Therefore, due to significantly reduced chemical background levels and despite the relative decrease in the analyte signal at higher concentrations, the IFT results were found to be characterized by 5–10-fold improvement in the LOD. Also,

increased ion statistics at the LOQ limit (see Figure 6, parts D and F) further improve system linearity at low analyte concentrations.

To summarize, the developed pulsed MRM approach has been found to offer several key figures of merit that make it a viable analytical tool. First, ion accumulation in an rf device, such as an IFT, at elevated pressures (>1 Torr) brings about additional desolvation of the ESI-generated droplets, as evidenced in the reduced chemical background levels and improved LOQ/LOD. Second, an increased charged density of the ion packets (due to ion accumulation) impinging on the detector produces more linear detector response in cases of low ion statistics and facilitate an improved linearity of the signal response as a function of the analyte concentration. Third, ion accumulation during the “dead” times between transitions increases the duty cycle of the IFT-QqQ instrument to unity.

CONCLUSIONS

We have developed a new pulsed MRM approach which was rigorously evaluated in capillary LC experiments with the complex biological sample such as a tryptic digest of *S. oneidensis* strain MR-1 spiked with several model peptides. As compared to the continuous mode of operation, whose sensitivity was further advanced with the introduction of an IF interface, the pulsed MRM approach is based on ion trapping at elevated pressures (>1 Torr) in the IFT followed by rapid release of higher charge density ion packets into a QqQ mass spectrometer. The use ofan IFT in conjunction with to a QqQ instrument was found to offer several analytical advantages. First, ion accumulation in the rf trap facilitates improved droplet desolvation, which is manifested in the reduced background ion noise at the detector. Second, signal amplitude for a given transition is enhanced by an order-of-magnitude increase in the ion charge density compared to the continuous mode of operation. Third, effectively full duty cycle in signal detection is obtained, as the use of the trap eliminates dead times between transitions, which are inevitable with continuous ion streams. In comparison with the conventional continuous mode of operation, the pulsed MRM signals yielded 5-fold enhanced peak amplitude and 2–3-fold reduced chemical background, resulting in an improvement in the LOD by a factor of ~4–8. Signal response as a function of the analyte concentrations for all the peptides under investigation showed excellent linearity over a wide range of analyte concentrations, suggesting the pulsed MRM approach as a viable tool for quantitative trace analyte analysis in highly complex biological matrixes.

Supplementary Material

Refer to Web version on PubMed Central for supplementary material.

Acknowledgments

The authors thank Drs. Erin Baker and Vladislav Petyuk for helpful discussion of experimental results. Portions of this research were supported by the U.S. Department of Energy (DOE) Office of Biological and Environmental Research, the Environmental Molecular Science Laboratory (EMSL), and the NIH National Center for Research Resources (Grant RR018522). This work was performed in the Environmental Molecular Science Laboratory (EMSL), a DOE national scientific user facility at the Pacific Northwest National Laboratory (PNNL). PNNL is operated by Battelle for the DOE under contract DE-AC05-76RL0 1830.

References

1. Mor G, Visintin I, Lai Y, Zhao H, Schwartz P, Rutherford T, Yue L, Bray-Ward P, Ward DC. Proc Natl Acad Sci USA. 2005; 102:7677–7682. [PubMed: 15890779]
2. Anglim PP, Galler JS, Koss MN, Hagen JA, Turla S, Campan M, Weisenberger DJ, Laird PW, Siegmund KD, Laird-Offringa IA. Mol Cancer. 2008; 7:62:1–13. [PubMed: 18179684]
3. Barry R, Soloviev M. Proteomics. 2004; 4:3717–3726. [PubMed: 15540209]

4. Yates JR, Ruse CI, Nakorchevsky A. Annu Rev Biomed Eng. 2009; 11:49–79. [PubMed: 19400705]
5. Chen CH. Anal Chim Acta. 2008; 624:16–36. [PubMed: 18706308]
6. Han XM, Aslanian A, Yates JR. Curr Opin Chem Biol. 2008; 12:483–490. [PubMed: 18718552]
7. Sechi S, Oda Y. Drug Discovery Today. 2004; 9:S41–S46.
8. Kitteringham NR, Jenkins RE, Lane CS, Elliott VL, Park BK. J Chromatogr, B. 2009; 877:1229–1239.
9. Lange V, Picotti P, Domon B, Aebersold R. Mol Syst Biol. 2008; 4:14.
10. Yates JR. Annu Rev Biophys Biomol Struct. 2004; 33:297–316. [PubMed: 15139815]
11. Domon B, Aebersold R. Science. 2006; 312:212–217. [PubMed: 16614208]
12. Hager JW, Le Blanc JCY. Rapid Commun Mass Spectrom. 17:1056–1064. [PubMed: 12720286]
13. Kenny DJ, Worthington KR, Hoyes JB. J Am Soc Mass Spectrom. 2010; 21:1061–1069. [PubMed: 20304673]
14. Unwin RD, Griffiths JR, Leverentz MK, Grallert A, Hagan IM, Whetton AD. Mol Cell Proteomics. 2005; 4:1134–1144. [PubMed: 15923565]
15. Stahl-Zeng J, Lange V, Ossola R, Eckhardt K, Krek W, Aebersold R, Domon B. Mol Cell Proteomics. 2007; 6:1809–1817. [PubMed: 17644760]
16. Ong SE, Blagoev B, Kratchmarova I, Kristensen DB, Steen H, Pandey A, Mann M. Mol Cell Proteomics. 2002; 1:376–386. [PubMed: 12118079]
17. Kuhn E, Wu J, Karl J, Liao H, Zolg W, Guild B. Proteomics. 4:1175–1186. [PubMed: 15048997]
18. Kapron JT, Jemal M, Duncan G, Kolakowski B, Purves R. Rapid Commun Mass Spectrom. 2005; 19:1979–1983.
19. Klaassen T, Szwandt S, Kapron JT, Roemer A. Rapid Commun Mass Spectrom. 2009; 23:2301–2306. [PubMed: 19579263]
20. Shaffer SA, Tang K, Anderson GA, Prior DC, Udseth HR, Smith RD. Rapid Commun Mass Spectrom. 1997; 11:1813–1817.
21. Belov ME, Gorshkov MV, Udseth HR, Anderson GA, Tolmachev AV, Prior DC, Harkewicz R, Smith RD. J Am Soc Mass Spectrom. 2000; 11:19–23. [PubMed: 10631660]
22. Wouters, ER.; Splendore, M.; Mullen, C.; Schwartz, JC.; Senko, MW.; Dunyach, JJ. Implementation of progressively spaced stacked ring ion guide on a linear ion trap mass spectrometer. Presented at the 57th Conference of the American Society for Mass Spectrometry; Philadelphia, PA. 2009.
23. Dodonov A, Kozlovsky V, Loboda A, Raznikov V, Sulimenkov I, Tolmachev A, Kraft A, Wollnik H. Rapid Commun Mass Spectrom. 1997; 11:1649–1656. [PubMed: 9364793]
24. Ibrahim Y, Tang KQ, Tolmachev AV, Shvartsburg AA, Smith RD. J Am Soc Mass Spectrom. 2006; 17:1299–1305. [PubMed: 16839773]
25. Ibrahim Y, Belov ME, Tolmachev AV, Prior DC, Smith RD. Anal Chem. 2007; 79:7845–7852. [PubMed: 17850113]
26. Ibrahim YM, Belov ME, Liyu AV, Smith RD. Anal Chem. 2008; 80:5367–5376. [PubMed: 18512944]
27. Clowers BH, Ibrahim YM, Prior DC, Danielson WF, Belov ME, Smith RD. Anal Chem. 2008; 80:612–623. [PubMed: 18166021]
28. Belov ME, Clowers BH, Prior DC, Danielson WF, Liyu AV, Petritis BO, Smith RD. Anal Chem. 2008; 80:5873–5883. [PubMed: 18582088]
29. Louris JN, Amy JW, Ridley TY, Cooks RG. Int J Mass Spectrom Ion Processes. 1989; 88:97–111.
30. Belov ME, Anderson GA, Wingerd MA, Udseth HR, Tang KQ, Prior DC, Swanson KR, Buschbach MA, Strittmatter EF, Moore RJ, Smith RD. J Am Soc Mass Spectrom. 2004; 15:212–232. [PubMed: 14766289]
31. Skov T, van den Berg F, Tomasi G, Bro R. J Chemom. 2006; 20:484–497.

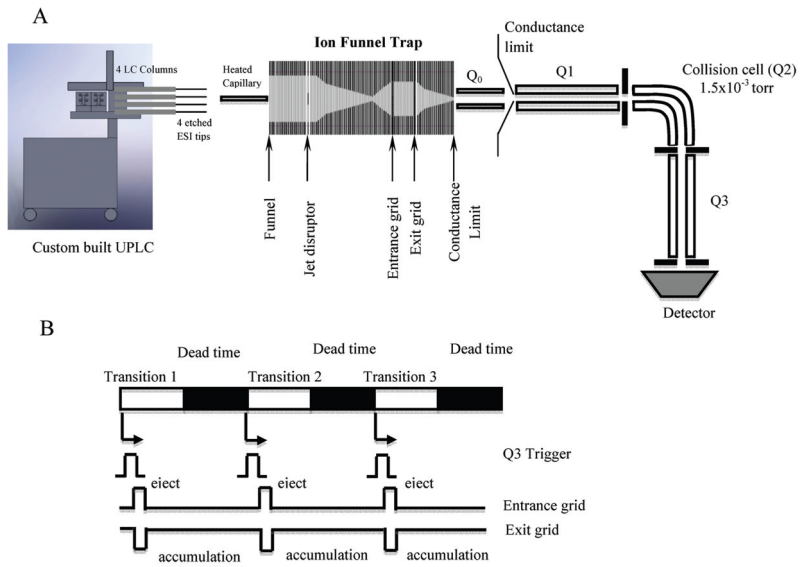

Figure 1.

(A) Experimental setup encompassing a custom-built HPLC and a triple-stage quadrupole (TSQ) equipped with an ESI–ion funnel trap (IFT) interface. The IFT operated at a pressure of ~1.0 Torr. (B) Experimental timing sequence, showing synchronization between the Q3 scan and an ion release from the IFT. The ion accumulation period was equal to the dwell time (2–50 ms) and switching time between transitions (4 ms).

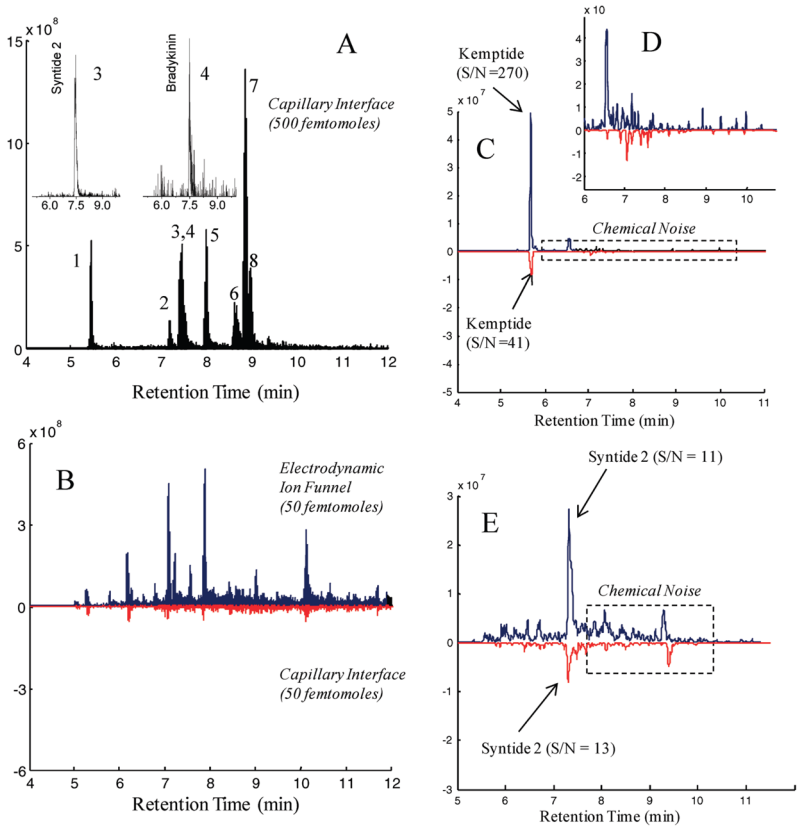

Figure 2.

(A) TIC from LC–MRM experiments with the commercial source, showing the elution of eight target peptides at ~500 fmol loaded onto the LC column. Each peptide peak is an integral of ion signals from three transitions. Insets show selected ion chromatograms (SIC) of coeluting syntide 2 and bradykinin. (B) Comparison of TIC acquired with LC–MRM using an electrodynamic ion funnel interface (IF, blue trace) and capillary–skimmer interface (red trace) of a sample that contains 10-fold less analyte as compared the to the sample represented in panel A. The matrix concentration was the same at 0.25 mg/mL for both panels A and B. (C and D) SIC corresponding to the elution time of kemptide ions. (C) Data obtained using the capillary–skimmer (red) and ion funnel interface (blue). (D) Expanded dashed area in panel C, representing chemical background. (E) SIC of syntide 2 for capillary–skimmer (red) and capillary–ion funnel (blue) interfaces.

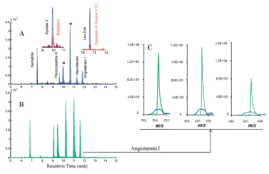

Figure 3.
LC–MS/MS analyses of a 0.25 mg/mL *S. oneidensis* tryptic digest spiked with eight peptides (500 fmol) employing ion funnel (A) and ion funnel trap (B) interfaces. The LC buffer included 0.2% HOAc and 0.05% TFA in water. (C) Comparison of MS spectra from three transitions of angiotensin I acquired with an ion funnel (blue) and ion funnel trap (green) interface.

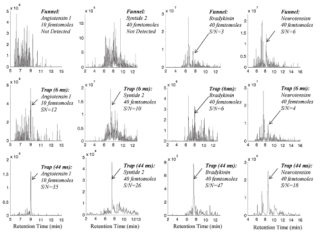

Figure 4.
Selected ion chromatograms from LC–IFT-MRM analysis of syntide 2, bradykinin, neurotensin (each at 40 fmol), and angiotensin I (10 fmol) with the ion funnel (top row) and ion funnel trap interfaces operating at accumulation times of 6 ms (middle row) and 44 ms (bottom row).

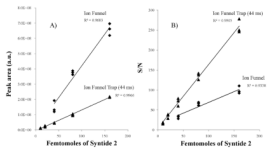

Figure 5.

(A) Regression analysis of the peak area as a function of the amount of syntide 2 loaded onto the LC column in the continuous (ion funnel) and pulsed modes (ion funnel trap). Data were obtained in the course of LC–IFT-MRM analyses of 0.25 mg/mL *S. oneidensis* tryptic digest spiked with eight reference peptides. In the continuous mode (IF), the regression analysis is shown in the concentration range between 40 and 160 fmol, as no signals were detected at peptide amounts less than 40 fmol. (B) Regression analysis for the same data set using S/N as a function of the peptide amount. See text for further details.

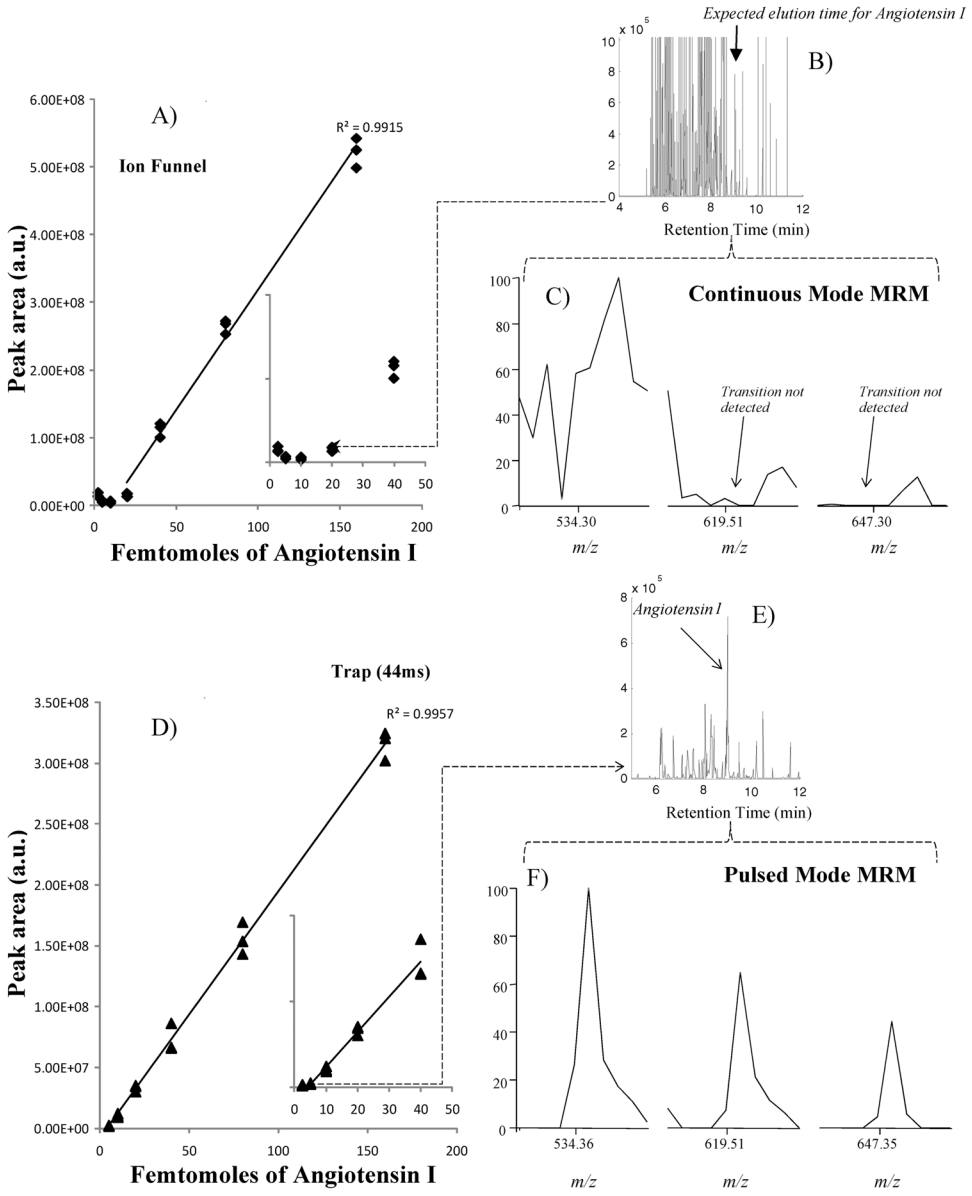

Figure 6.

Peak area as a function of the angiotensin I amount loaded onto the LC column in the continuous (A) and trapping (B) modes. Peak areas were derived by summing signals from the three most abundant transitions. Each data point in the plot corresponds to a separate LC–IF-MRM run. (B) Selected ion chromatograms (SIC) and the corresponding transitions of angiotensin I at 20 fmol acquired in continuous (B and C) and trapping (E and F) modes.